Design, commissioning and performance of a device to vary the turbulence in a recirculating flume

Luke Myers*[#1], Khilan Shah[#2], Pascal Galloway[#3],

[#]*Sustainable Energy Research Group, Faculty of Engineering and the Environment, University of Southampton, Southampton, SO17 1BJ, UK.*

[1]L.E.Myers@soton.ac.uk

[2]K.D.Shah@soton.ac.uk

[3]P.W.Galloway@soton.ac.uk

[*]*Corresponding author. Tel: +44(0) 2380593946*

Abstract— **Ambient turbulent flow structures are one of the key drivers that will determine the rate of wake recovery downstream of tidal turbines. For second and third generation arrays or farms such a parameter is critical for the determination of inter-device spacing and the optimisation of energy extraction per unit surface area. At present offshore flow characterisation is dominated by seabed or surface-mounted diverging-beam acoustic Doppler profilers that whilst having a good spatial capture cannot characterise turbulent flow structures to the same accuracy as single point converging laboratory-scale velocimeters. So a paradox presently exists: We can measure the (mean) flow characteristics at real tidal energy sites but lack the ability to accuracy ascertain high-frequency flow characteristic at discrete spatial locations. This is possible at laboratory-scale with convergent-beam devices but as we do not know the real site conditions replication at small-scale can only be approximated.**

To date there has been few laboratory studies where the ambient flow turbulence has been varied. The standard method is to generate turbulence from a static structure such as a grid. Here we have developed an articulated rig that has the ability to oscillate cylindrical members along two axes in the flow upstream of tidal turbine models. Initial results presented in this paper show the effect upon the ambient flow that the turbulence-generating rig can impose and the effects upon wake dissipation for varying levels of turbulent length and time scales. Also the formation and insistence of turbulent structures shed from the device are reported. As expected increasing ambient turbulence intensity serves to dissipate the turbine wake more rapidly and whilst we cannot directly relate these laboratory flow characteristics to full-scale tidal energy sites at present it is hoped that offshore measurement technology and that of laboratory replication can converge so that device performance prediction can be performed at smaller-scale and at a corresponding lower cost to the technology.

Keywords— **Tidal turbine, wake, turbulence, wake recovery,**

I. Introduction

There are a number of variables that govern the characteristics of the wake generated by a tidal turbine and its rate of dissipation. Purely device-driven parameters include efficiency/rate of energy extraction (usually expressed as dimensionless thrust and power coefficients), the area over which energy is captured (usually rotor diameter), the location of the energy capture within the water column and the nature of the device supporting structure which will generate a wake that will interact with that generated by the power capture subsystem (rotor). Combined device/environment parameters include rotor diameter/water depth ratio and the direction of inflow to the power capture subsystem. Purely environmental driven parameters include inflow velocity (one of the terms in the dimensionless Froude and Reynolds numbers) and the nature of turbulence which can be generated from a number of sources as shown in Fig. 1.

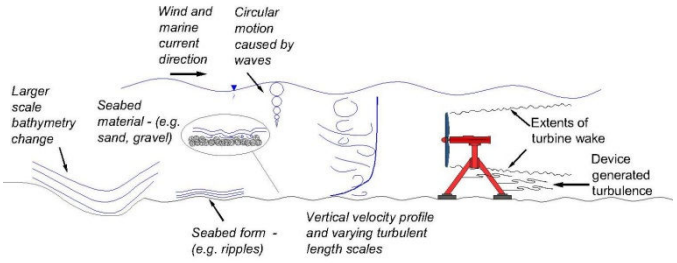

Fig. 1 Sources of turbulence around a tidal turbine

Offshore velocity measurement is dominated by Acoustic Doppler Current Profilers (ADCPs). Current profilers measure current speed and direction in multiple layers throughout the water column. Units can be mounted on the seabed in an up-looking configuration or down-looking from either a vessel or surface buoy. Acoustic beams diverge from the ADCP unit to form a conical volume. Average velocity and direction is measured at discrete distances from the ADCP using timed data collection within each pulse of acoustic energy. Advantages of the technology include the good spatial collection of data through the water column and the position in the lowest velocity of the flow if mounted on the seabed. Acquisition frequency is not high with the latest units emitting acoustic pulses at 10Hz but often averaging over several pulses is required to reduce standard deviation of the velocity in each vertical cell. As the acoustic beams diverge, the vertical cells increase in volume further way from the instrument meaning it is not well-suited to accurately

quantifying turbulence intensities or characterising flow structures.

At laboratory scale converging beam Doppler velocimeters are commonly used either employing sound (Acoustic Doppler Velocimeter, ADV) or light (Laser Doppler Velocimeter, LDV) and measuring the Doppler shift of the retuned signal. Sample rate is high; a few hundred Hz for ADVs and several thousand Hz for LDVs. Turbulence intensities can be accurately quantified alongside dominant length scales from very small sample volumes. However flow characterisation requires multiple single point measurements to be acquired thus the temporal characteristics of these instruments is not favourable. The requirement to place the instrument close to the region of flow that is being measured means that deployment in this deployment in deep, fast-moving waters offshore is not practical. Thus a dichotomy exists between lab and field measurement technology.

There have been a number of studies at sites with strong tidal flows especially since the tidal energy industry has seen significant development. Thomson et al. [1] conducted a comparison of ADCP and ADV when deployed in a tidal channel. The ADV was mounted on a frame 2.5m vertically above the ADCP allowing direct comparison of the ADV with the relevant measurement bin from the ADCP. Turbulence intensities were quantified as 10 and 11% from the ADCP and ADV respectively following removal of the Doppler noise which has a strong effect upon estimates of higher order flow effects when calculated from a limited number of pings. Turbulence dissipation rates differed by 2-orders of magnitude, the cited reason for poor disagreement was the strong influence of Doppler noise and at stronger tidal flows velocity fluctuations were small. A similar study was conducted by Milne et al. [2] whereby an ADV was mounted within the measurement volume of an ADCP. Turbulence intensities 5m above the seabed were found to be 12-13% in the streamwise direction, 9-10% and 7-8% in the transverse and vertical directions respectively. Along with other higher-order flow characteristics this gives a good indication as to where smaller-scale experiments can really benefit the technology with regards to reproducing a representative flow field.

II. Experimental Set-up

A. Apparatus & Settings

The turbulence generator rig was realised from the need to generate controllable and persistent turbulent flow features in circulating flumes and channels. Previous work conducted by the group has investigated many of the variable affecting the wake generated by a small-scale tidal turbine including rotor thrust coefficient, Froude number, position of device in the water column [3] and wake interaction between adjacent devices [4] but experimental variation of the free stream turbulence has not seen a great deal of work. The most useful study was conducted by Maganga et al. [5] in a large circulating water channel. The downstream wake from a 0.7m-diameter horizontal axis turbine was comprehensively measured for ambient turbulence intensities of 5% and 14%. (These are the turbulence intensity values as defined in Equation 2a, a slightly different definition is used by Maganga et al.). The variation in turbulence intensity was due to the removal of flow-straightening elements in the channel and so not strictly controllable in terms of axial components or length scales. However the research did quantify the significant effect that the ambient turbulence has upon downstream wake recovery of tidal turbines.

The standard method of changing ambient turbulence levels of a fluid under experimental conditions is similar to that described above whereby a static grid element is introduced or the geometry of this mesh or grid is altered. Such an approach has seen good usage in wind tunnel experiments [6] but active-grids have also been developed with dynamic elements such as ones shown by Matika [7] and Mydlarski and Warhaft [8]. These consisted of a grid of bars with triangular wing attachments that could flap in a random or defined manner and were used in order to investigate properties of turbulence at various Reynolds numbers.

For an active grid for use within a flume a different design was required due to the nature of the tidal current flow behaviour trying to be replicated and the physical limitations of the flume. The turbulence generator was designed for use in the large tilting flume at the Chilworth hydraulics laboratory, University of Southampton. The flume working section is 21m in length, 1.35m wide and can operate at depths up to 0.5m. The bed is relatively smooth render and sidewalls are toughened glass.

Fig. 2 shows the generator which is composed of two grid elements aligned orthogonal to the principle flow direction. Two independent servo drives oscillate the elements; the vertical (red in Fig. 2) elements move in a cross flume direction whist the horizontal elements oscillate vertically through the water column. Stroke length, rate and acceleration can be varied along with the number and shape of the elements.

The initial set of commission runs were performed only using the vertical ‘rake’ moving in the lateral (cross-flume) direction as shown in the lower half of Fig. 2. This lateral rake consisted of 6 elements with a rectangular cross section of 20x10mm spaced 150mm apart. The clearance between the elements and the bed was in the order of 10mm. The lateral movement was set to traverse across the flume and back (one complete cycle) at 0.39 Hz, moving a distance of 305mm in each traverse. The centre of the flume experienced six wakes shedding off the elements in each cycle, thus a ‘forcing frequency’ at flume centre is approximately 2.4Hz.

In line with previous work taken place at the University of Southampton, single tidal turbine devices have been simulated using porous ‘actuator’ disks 100mm in diameter. Whilst these porous disks are not able to simulate the swirl component of the near wake, far wake properties have been shown to be representative of horizontal axis turbines [9]. Disks were held in position using thin section stainless steel bar passing through a pivot point located above the water line. This pivot arrangement mechanically amplified the thrust

force on the disks which was then measured using low range load cells. Full details of this apparatus is described in [3].

Fig. 2 CAD assembly and image of turbulence generator operating in flume

High frequency flow velocity measurements were acquired using a downward-facing Nortek Vectrino ADV mounted to a 2-axis automated positioning rig. General flow measurements were acquired at 50Hz for duration of 180 seconds giving 9000 data points. From this mean velocity, turbulence intensity and shear stresses were quantified. Measurement of turbulent length scales were acquired over 20 minutes giving 60000 discrete data points.

B. Experimental Procedure

The inlet to the 21m flume is not of an optimal design. Two large-bore supply pipes introduce water vertically downwards into a small volume sump positioned below the working section. This water rises up driven by a reduction in hydrostatic head from the inlet to outlet. The flow close to the inlet of the working section is therefore highly rotational and as such takes a reasonable time or length along the working section to become steady in terms of vertical velocity profile and turbulence intensity. It was important to ensure that the added turbulence generated was introduced into a relatively stabilised flow field. If installed close to the inlet then any generated turbulence might be overcome by the ambient flow with generated turbulent structures difficult to characterise. Two sets of honeycomb flow straightening elements were installed in the working section close to the inlet to reduce the length required for stabilised flow with the turbulence generator positioned close to the leading edge of this steady region. Total water depth was 0.3m, depth-averaged flow velocity was approximately 0.3m/s. For the first set of commissioning experiments only the stroke rate (frequency of oscillation) was varied.

For models approximating tidal channels it is important to maintain parity in the non-dimensional Froude and Reynolds numbers. As the tidal turbine rotors operate in a relatively shallow flow it is important that the model does not have a high Froude number that can lead to unsteady water surface profiles. The Reynolds number, the ratio of inertial to viscous forces is also important as tidal channels operate in a fully developed turbulent flow. Faithfully maintaining parity for both parameters is not possible at smaller scales so it is generally accepted that as long as the Reynolds number is in the fully turbulent regime, Froude parity should be held to prevent non-realistic surface deformations. The shape of the vertical velocity profile demonstrates a fully-turbulent flow and is shown in [3].

C. Data Handling

Doppler velocimeters can suffer from data errors originating from Doppler noise, low return signal strengths, acoustic pulse reflection errors (when subsequent acoustic pulses cross in the sample volume leading to increased sample energy) entrained air in flows and data aliasing (often arising from poor instrument set up). The use of seeding material and the hard water present at Southampton results in a high signal feedback that limit many of the aliasing errors and lead to very strong return signal strengths however spikes in the samples can still be present. To this end data was filtered to remove any such spurious spikes using a velocity cross correlation filter [10]. This filter has been used previously by the authors and generally less than 2% of the sample set is affected meaning that sample sets can be truncated rather than employing data replacement techniques which are difficult to justify as they require user-define parameters to be set.

The remaining sample readings were then processed to calculate the mean velocity in all 3 planes and the corresponding turbulence intensities as normalised by the mean velocity.

All velocity measurements downstream of the scaled actuator disks were normalised against those existing upstream of the rotor plane. This is expressed by a dimensionless parameter the velocity deficit, U_{def} by:

$$U_{def} = 1 - \frac{U_w}{U_0} \tag{1}$$

Where U_w and U_0 are the measured wake and rotor plane inflow velocities respectively. Turbulence intensity, I is defined as the root-mean-square of the turbulent velocity fluctuations with respect to the mean velocity and is calculated by Equation 2a.

$$I = \frac{\sqrt{\frac{1}{3}\left(\langle u_x'^2\rangle + \langle u_y'^2\rangle + \langle u_z'^2\rangle\right)}}{\sqrt{U_x^2 + U_y^2 + U_z^2}} \tag{2a}$$

$$I_i = \sqrt{\frac{\langle u_i'^2 \rangle}{U_x{}^2 + U_y{}^2 + U_z{}^2}} \quad (2b)$$

It follows that expressions for intensity along each component can also be defined as shown in Equation 2b, where u'_i is the fluctuating velocity component for i = x,y,z (longitudinal, lateral and vertical components respectively).

The shear stress can be used to analyse the rate of mixing between adjacent fluid streams. For example in the flume at a distance far from the inlet and close to the centre of the working section the horizontal mixing is expected to be close to zero whilst the vertical mixing will be most prevalent close to the bed within the sheared boundary layer. The horizontal and vertical components of shear stress can be expressed as:

$$Horizontal\ shear\ stress = -\rho < u'_x u'_y > \quad (3)$$

$$Vertical\ shear\ stress = -\rho < u'_x u'_z > \quad (4)$$

Turbulent length scales were an important addition to the turbulence intensity in understanding the nature of the structures within the flow. The approximation of spatial correlations by temporal correlations is known as Taylor's hypothesis [10]. This technique allows data recorded with a single stationary probe to be analysed as if it were a series of spatial measurements. The integral time scale is a measure of how long the largest energy containing eddies stay correlated for and the integral length scale is a measure of the size of these eddies, The method for calculating these scales is very well explained by Milne et al. in [2] and uses the normalised autocorrelation function which is defined as:

$$R_{ii}(s) = \frac{\langle u'_i(t) u'_i(t+s) \rangle}{\langle u'_i(t)^2 \rangle} \quad (5)$$

Where t is time step and s is lag. To find the integral timescale of the flow, T_i, the autocorrelation function is integrated with respect to time between the limits of s=0 and the value for s where the first instance of $R_{ii}(s) = 0$ as shown in Equation 6 below:

$$T_i = \int_{s=0}^{s(R_{ii}(s)=0)} R_{ii}(s) ds \quad (6)$$

and in turn is related to integral length scale, L_{ii} by:

$$L_{ii} = T_i U \quad (7)$$

where i can be substituted with the direction in question, x, y, or z and U is the 3D velocity magnitude at the point measured.

Integral length scales are constrained by the characteristic length of the flow such as the width of the flume for the ambient flume flow or the distance between vertical mixing elements on the turbulence generator. These length scales pertain to eddies that contain the most energy.

Finally the brief investigation of the one dimensional energy spectra [6][11] allows further investigation of the effect of the turbulence generator on the flow. The one dimensional energy, E_{ii}, is closely related to the auto correlation function (Equation 5) and makes the following Fourier transform pair:

$$E_{ii}(\omega) = \frac{2}{\pi} \langle u_i'^2 \rangle \int_0^\infty R_{ii}(s) \cos(\omega s)\, ds \quad (8)$$

$$R_{ii}(s) = \frac{1}{\langle u_i'^2 \rangle} \int_0^\infty E_{ii}(\omega) \cos(\omega s)\, d\omega \quad (9)$$

where ω is the frequency and s is the lag.

III. Experimental Results & Discussion

A. Development of ambient flow in flume

The vertical velocity profile generated in the flume under ambient conditions (reported in [3]) is well-developed, fully turbulent in nature and shape, with an approximate 1/8th-power law profile from bed to mid-depth and constant velocity up to the water surface.

Figure 3 shows measured flow data for a vertical plane running down the longitudinal axis of the flume. It can be seen that after approximately 7m the velocity and turbulence intensity along the longitudinal x-direction becomes steady with respect to depth. The turbulence in the lateral and vertical planes showed similar growth and development also becoming steady at 7m from the inlet.

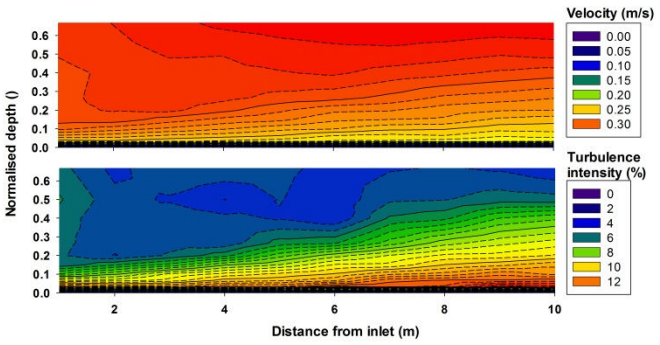

Fig. 3 Longitudinal velocity and turbulence intensity in flume running empty

The turbulence generator was installed at a distance of 7m from the inlet of the working section. For reference the mid-depth x, y, z ambient turbulence intensities from 7m onwards were 5.5 - 5.8%, 4 - 5% and 2.2 - 2.8% respectively.

B. Persistence and characteristics of added generated turbulent flow as compared to ambient flow

Figure 4 shows the development of turbulence intensity from the generator along a longitudinal axis located at channel mid-depth and mid-width. Naturally the lateral motion of the elements immersed in the flume cause the greatest increase to the turbulence intensities in the x and y direction. At 4m from the generator the ratio of intensity (x: y: z) is 1: 0.96 : 0.67 which is similar to that observed in the sound of Islay [2] although it is acknowledged that this ratio and the magnitude of turbulence will no doubt be highly site-specific. However it does demonstrate that this sort of active turbulence generation can be tuned to closely represent length scales and turbulence intensities at real tidal sites. The number and shape of oscillating elements, stroke rate and length can all be varied as can the plane of oscillation. This means the generator has the potential to produce a wide range of flow conditions.

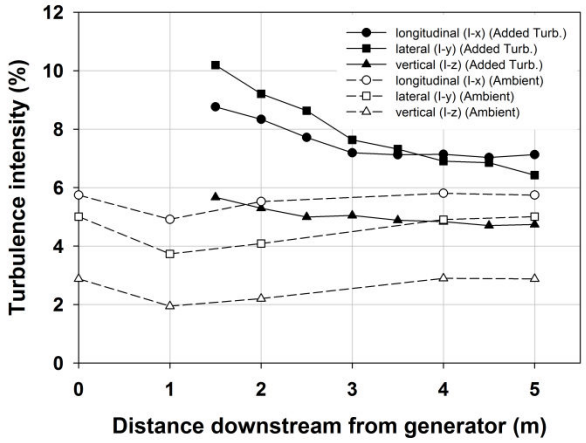

Fig. 4 Centre flume turbulence intensities (I_x, I_y, I_z) downstream of the turbulence generator for ambient (dashed line) and added turbulence (solid line) conditions.

A further key observation from Fig. 4 is the relative stability of the turbulence intensities between 3 and 5m downstream of the generator (solid lines). This equates to 20-acturator disk diameters (at the scale employed here) which is adequate for the wake produced by the disk to almost completely dissipate in a relatively stable flow field. The additional turbulence generated from the rig is clear by the comparison of the solid and dashed lines. It is noted that the peak turbulent intensity 1.5m away from the generator is smaller in value than the higher turbulence intensity produced by Maganga et al. [5]. This can be attributed to the different method of turbulence generation and difference in flume type. The flume used in [5] is a closed circulating tunnel type (analogous to a closed-loop wind tunnel) with the pump acting directly on the flow upstream of the working section. Once the flow straighteners are removed the work done by the pump and the curvature of the water tunnel allows for a higher turbulence intensity to be seen in the working section. The Chilworth flume operates a gravity fed system with the water pumped through two large bore pies that fill a sump upstream of the working section as explained in section II B. Thus this flume design removes the turbulence generated by the pumps and the additional honeycomb structures reduce the turbulence from the gravity fed section. There is also a natural break at the outlet as water falls into the sumps which means no objects placed in the working section can influence the inflow to the working section with regards to added turbulence etc.

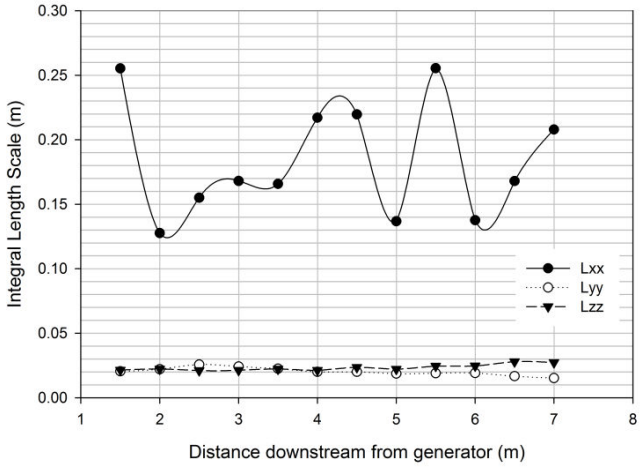

Fig. 5 Integral length scales, L_{xx}, L_{yy}, L_{zz} for ambient flow conditions

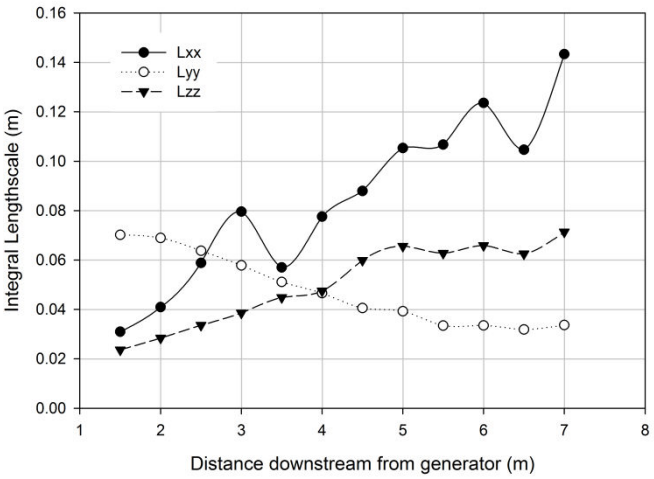

Fig. 6 Integral length scales, L_{xx}, L_{yy}, L_{zz} for added turbulence condition

Fig. 5 shows the integral length scales, L_{xx}, L_{yy}, L_{zz} for the ambient flow condition. Though quite scattered, the general value for L_{xx} seems to be between 0.15 and 0.2m and this is fairly consistent throughout the measured section. L_{yy} and L_{zz} show very little scatter and are very stable. This suggests that the large scale eddies in the flow are fully developed and are already being constrained by the physical boundaries of the flume. As the overall turbulent kinetic energy in the ambient flow is already low, small differences in the mean flow (which

is in the x-direction) and fluctuating velocities are likely to be amplified, leading to the larger degree of scatter observed.

The integral length scale measurements for the added turbulence case, Fig. 6, show the development of the flow behind the generator. The lateral length scale, L_{yy}, is the largest length scale directly behind the generator due to the energy being added to the water through lateral motion. As the flow develops, this motion dissipates and seems to transfer energy to the larger scales in the streamwise and vertical direction. As the flow develops, the value of L_{yy} is seen to fall to approximately those seen in the ambient flow in Fig. 5. L_{xx} and L_{zz} are seen to grow behind the generator. By the end of the measured section, L_{xx} is approaching the size seen in the ambient flow, however L_{zz} seems to grow beyond the ambient case. This could be due to the establishment of a new boundary layer at the location of the turbulence generator.

It is important to show that the turbulence generator rig is capable of producing repeatable results. This can be seen in Fig. 7 where lengthscale measurements from 3 separate runs with additional turbulence performed on different days (but same experimental settings) are plotted with the ambient results shown for reference. There is very good agreement with all three runs and trend of a growing L_{xx} is well established as expected behind an active grid.

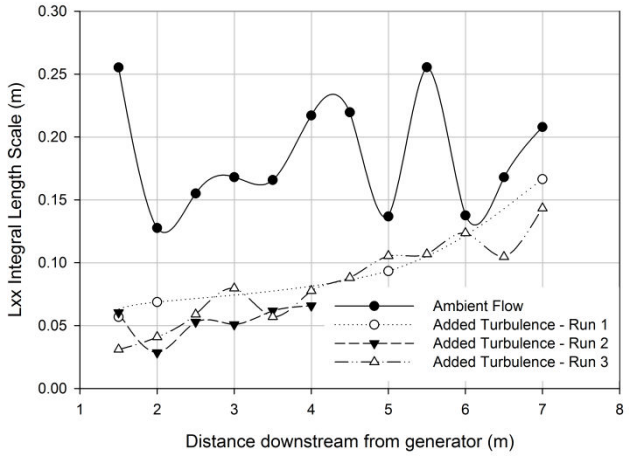

Fig. 7 Repeatability of lengthscale measurements – L_{xx} measurements for ambient flow and repeated experiment runs with added turbulence

The actuator disk was installed 2m downstream of the turbulence generator (see section III C). The disk was 0.1m diameter and located at centre-depth and width of the flume. From the above figures it is clear that while the integral length scales are smaller in the ambient turbulence cases, the energy contained within the flow is much greater as shown by the higher turbulence intensity. This higher energy was expected to have a significant effect upon wake dissipation downstream of the actuator disk.

Fig. 8 shows the one dimensional energy spectrum (Equation 8) plots, smoothed by using a 5 point average, in all three components (streamwise = 11, transverse = 22, vertical = 33) at the actuator disk location but in its absence. It is clear for all three directional components that the added turbulence provides more energy at the lower frequencies, which correspond to the larger eddies in the flow. Fig. 8(c) shows a marked increase in energy in the vertical direction, much larger than that of the streamwise or transverse flows. This, together with the downstream development of the integral length scales (Fig. 6), suggests that the added energy in the tranverse directions from the generator is being transferred to both the streamwise and vertical components of the flow. The inertial sub-range [11] is well captured in all three plots at higher frequencies as shown by the gradients of approximately -5/3.

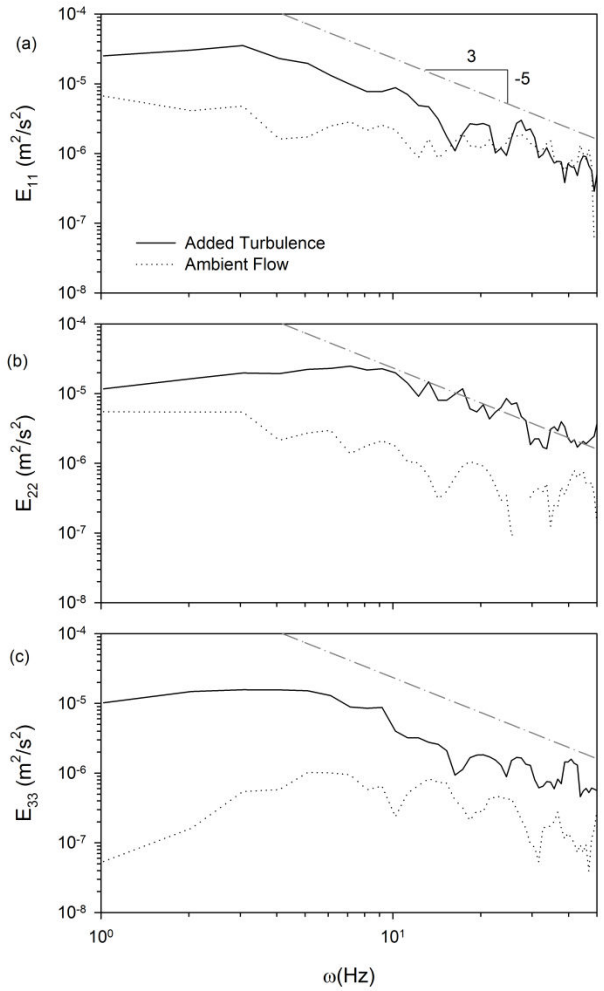

Fig. 8 One-dimensional energy spectrum plots, E_{11}, E_{22}, E_{33} at the disk location for both ambient flow and added turbulence conditions, where solid line represents added turbulence flow, dotted line represents ambient flow, and dot-dash line represents -5/3 gradient.

It is noted that the plots shown in Fig. 8 are fairly crude and display much noise at higher frequencies and are limited by the sample rate used. However they provide a useful insight into the behaviour of the turbulence being generated, future work will look to further analysing the turbulent behaviour behind the generator in more detail.

C. Effect upon tidal turbine wake dissipation

A model actuator disk was installed downstream of the turbulence generator and flow measurements acquired in the downstream wake along an axis through the centre of the disk. Fig. 9 shows the downstream velocity deficit for two flow cases of the ambient flume flow (quantified in section III A) and with the turbulence generator oscillating vertical elements in a lateral sense (quantified in section III B). Inflow velocities to the disk in the ambient flow case were measured in its absence as 0.33m/s. With the added turbulence, this reduced slightly to 0.30m/s however the normalised rate of wake recovery has been shown to be independent of inflow velocity for Froude numbers expected at tidal turbine sites [3].

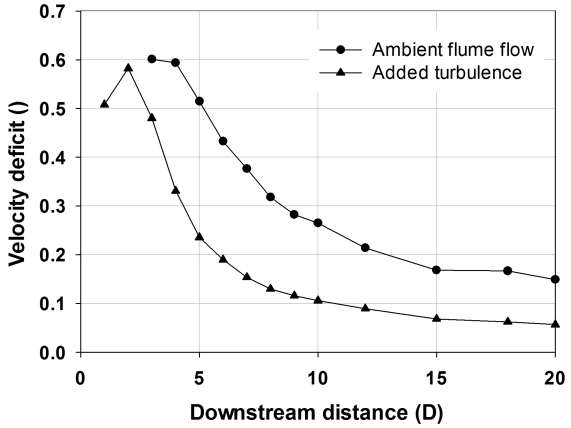

Fig. 9 Downstream centre line wake velocity deficit of an actuator disk for two flume turbulence intensities

From Fig. 9 the difference in wake recovery is apparent and demonstrates the influence of the turbulent structures present in the incoming flow to the rate of dissipation of a tidal turbine wake. The initial rate of recovery is much greater for the added turbulence case in the near wake region and up to approximately 7-diameters downstream at which point both recovery rates show a similar trend. Power capture is proportional to the cube of velocity; at an arbitrary downstream location 10 diameters downstream a tidal turbine would be able to capture over twice as much energy for the higher turbulence case. For large arrays Fig. 9 illustrates the importance of quantifying the inflow turbulence so that turbines can be optimally spaced especially when operating within the wake of an upstream device.

Investigation of the wake turbulence intensities (Fig. 10) go some way to explaining the rate of wake recovery. For the higher turbulence case there is a clear increase in turbulence in the near wake indicating ambient flow features combining with those generated from the actuator disk increasing the rate of fluid mixing and hence leading to a much more rapid recovery in centreline velocity. Further downstream the rate of change in turbulence intensity is much more similar suggesting a similar rate of wake recovery as observed in Fig. 9. It can be seen that it takes a short downstream distance for the ambient flow features to penetrate to the centreline of the wake and that the more-energetic structures in the added turbulence case achieve this closer to the disk as indicated by the peak turbulence intensities on the plots in Fig. 10.

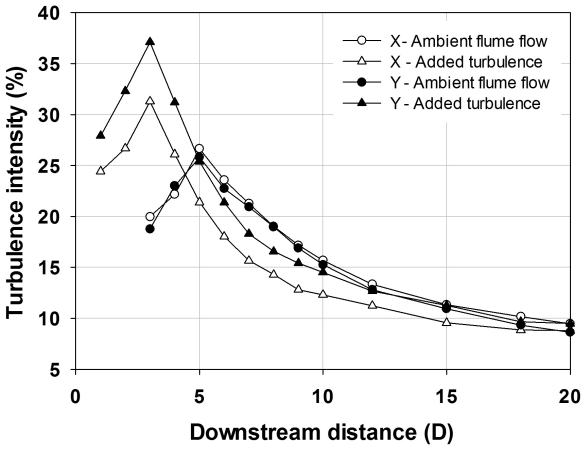

Fig. 10 Downstream centre line wake longitudinal and lateral turbulence intensities in the wake of an actuator disk

Fig. 11 shows the normalised XY-plane shear stress along the centreline of the wake in both cases. Here the shear stresses have been normalised by the square of the mean velocity measured at each point. Generally higher shear forces arise from a greater differential velocity between two adjacent fluid streams and the increased wake recovery in the near wake region can be explained in some way by this parameter. The horizontal shear is much greater in the near wake for the added turbulence case meaning that momentum is being transferred from the ambient flow moving around the disk to the more stagnant wake flow promoting a more rapid recovery in wake velocity.

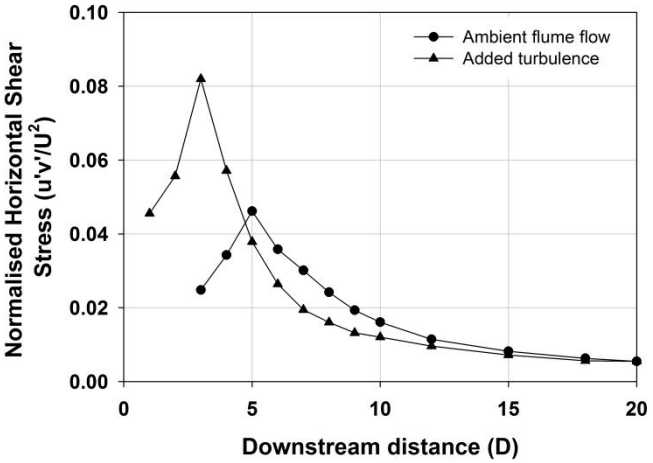

Fig. 11 Downstream centre line normalised lateral horizontal shear stress in the wake of an actuator disk for two flume turbulence intensities

The results of this initial experiment presented here are quite similar to those addressed in [4] where the near wake recovery of a scale tidal turbine is more heavily affected by increasing ambient turbulence whilst the far wake shows a

similar rate of recovery albeit at different absolute magnitudes. Work will continue to commission and map the performance of the turbulence generator with regard to characterising the generated flow field.

IV. Conclusions

This paper details the design, commissioning and performance of an active turbulence generator for use in large circulating flumes. When installed in a stabilised (with regard to flow properties along the longitudinal flume axis) flow field the generator can create more turbulent flow structures that can persist in a relatively steady manner over a distance sufficient to conduct small-scale experiments into the wake recovery of tidal turbines. Initial results show that for an ambient flow with more-turbulent structures the downstream wake recovery is much enhanced which has implications for design of tidal turbine arrays and inter-device spacing within them. More turbulent flow penetrates more rapidly to the centreline of the wake enhancing fluid mixing and leading to a much faster initial recovery in velocity followed by a reduced deficit further downstream.

On-going work will aim to better-characterise the turbulent structures generated and quantify their effects upon single device performance and that of different array configurations. The nature of the wake flow will also be quantified in higher spatial resolution in all 3 planes downstream to gain a better understanding of both intensity and length scales influence wake recovery. With the improvement of offshore velocity measurement technology and understanding of the methods that can be employed to advance the accurate characterisation of transient flow structures it is hoped that this active generator used at smaller scale can be used to inform tidal turbine array design at different sites.

Acknowledgement

This work was funded by the Royal Society grant number RG110369.

References

[1] J. Thomson, B. Polagye, M. Richmond, V. Durgesh "Quantifying turbulence for tidal power applications" MTS/IEEE Seattle, OCEANS September 20 -23, 2010.

[2] I. Milne, R.N. Sharma, R. G. J. Flay, S. Bickerton "Characteristics of the turbulence in the flow at a tidal stream power site" Philosophical Transactions of the Royal Society A: Mathematical, Physical and Engineering Sciences, v 371, n 1985, 2013.

[3] L.E. Myers and A.S. Bahaj, "Experimental analysis of the flow field around horizontal axis tidal turbines by use of scale mesh disk rotor simulators" Ocean Engineering, vol. 37, pp.218-227, February 2010.

[4] L.E. Myers and A.S. Bahaj, "An experimental investigation simulating flow effects in first generation marine current energy converter arrays," Renewable Energy, vol. 37, p 28-36, January 2012.

[5] F. Maganga, G. Germain, J. King, G. Pinon, E. Rivoalen "Experimental characterisation of flow effects on marine current turbine behaviour and on its wake properties" IET Renewable Power Generation, v 4, n 6, p 498-509, November 2010.

[6] P. Krogstad and P. A. Davidson, "Freely decaying, homogeneous turbulence generated by multi-scale grids," J. Fluid Mech., vol 680, pp.417-434, May 2011.

[7] H. Matika, "Realization of a large-scale turbulence field in a small wind tunnel," Fluid Dyn. Res. vol. 8, pp.53-64, October 1991.

[8] L. Mydlarski and Z. Warhaft, "On the onset of high-Reynolds-number grid-generated wind tunnel turbulence," J. Fluid Mech., vol. 320, pp.331-368, August 1996.

[9] P.M. Sforza, P. Sheerin and M. Smorto, "Three-dimensional wakes of simulated wind turbines" AIAA Journal, vol. 19, no. 9, pp.1101-1107, September 1981.

[10] L. Cea, J. Puertas and L. Pena, "Velocity measurements on highly turbulent free surface flow using ADV," Experiments in Fluids, vol. 42, no. 3, pp.333-348, March 2007.

[11] S.B. Pope, Turbulent flows, Cambridge University press, Cambridge (2000).